CONJUGATE JET IMPINGEMENT HEAT TRANSFER INVESTIGATION

Nasif G.*, Barron R. M., and Balachandar R.
*Author for correspondence
Department of Mechanical, Automotive and Materials Engineering,
University of Windsor,
Windsor, ON,
Canada,
E-mail: nasifg@uwindsor.ca

ABSTRACT

A transient numerical investigation has been carried out in this study to evaluate the effects of the conjugate heat transfer (CHT) onto the thermal characteristics due to the air and water jet impingement process. It is shown that the convective heat transfer at the fluid-solid interface is influenced by the nozzle size, boundary heat flux and thermal conductivity of the metal. The thermal characteristics from the CHT process approaches the one with no CHT process as the thermal conductivity of the metal decreases. One of the important effects of the CHT process is to redistribute the uniform boundary heat flux inside the solid and create a non-uniform heat flux boundary at the fluid-solid interface.

INTRODUCTION

Many industrial applications are subjected to a strong thermal interaction between fluids and solids. Conjugate heat transfer (CHT) is thus an essential issue in the industry, which can be verified in different ways. Analytical methods generate good results to identify the main parameters of the problem and to validate the codes. However, the applications of the analytical methods are restricted to very simple configurations [1-5]. Experiments, which are an approach to the analytical methods, are significantly expensive and cannot be relied on in the industry. The modern computational CHT was developed after computers came into a broad application to substitute the empirical expressions of proportionality of heat flux to temperature difference with heat transfer coefficient (HTC). The state-of-the-art of the computational method involves coupling the conduction in the solid and convection in the fluid to predict the HTC at the interface. The coupled approach is more reliable and common than a decoupled solution [1]. In the computational CHT approach, two separate simulations are set up, one for fluid analysis and another for solid thermal analysis. Assuming the temperature distribution on the wall boundary, the fluid flow problem is solved to determine the local HTC distribution on the wall. The HTC distribution with the reference temperature is applied to the solid thermal simulation to re-evaluate the temperature distribution in the solid. The wall temperature distribution predicted by the solid thermal analysis is fed back to the transient flow simulation and applied as a wall boundary condition to re-evaluate the modified HTC distribution. The iteration process continues until the solution is obtained with a suitable accuracy.

The objective of the current study is to investigate the effect of the CHT process on the convective heat transfer coefficient due to the jet impingement process. For this end, numerical simulations are performed using circular air and water jets, impinging vertically on a heated flat plate with different thicknesses and materials

NOMENCLATURE

A	[m^2]	Control volume surface are
c_p	[J/kg.K]	Specific heat
D	[m]	Disc diameter
d	[m]	Nozzle diameter
H	[m]	Nozzle-to-target spacing
k	[m^2/s^2]	Turbulent kinetic energy
n	[-]	Unit normal vector
Nu	[-]	Nusselt number
q	[W/m^2]	Heat flux
r	[m]	Radial distance from stagnation point
R	[m^{2}K/W]	Thermal resistance
Re	[-]	Reynolds number
S	[-]	Source term
t	[s]	Time
T	[°C]	Temperature
u	[m/s]	Velocity vector
V	[m/s]	Bulk velocity
$y+$	[-]	Non-dimensional wall distance

Special characters

$\Gamma_\emptyset$	[-]	Diffusion coefficient (μ or κ)
Δ	[-]	Delta
κ	[W/m.K]	Thermal conductivity
ρ	[kg/m^3]	Density
$\emptyset$	[-]	Transported scalar property per unit mass
ω	[1/s]	Specific turbulence dissipation rate

Subscripts

A	Surface
a	Axial direction
b	Boundary
CV	Control volume
i	Fluid-solid interface
j	Jet
r	Radial or transverse direction
0	Stagnation point
$\emptyset$	Transported property

NUMERICAL METHOD

In the current study, the jet impingement process is modeled using CD-adapco's STAR-CCM+ commercial code [6]. First-order implicit time marching and second-order spatial differencing are employed to discretize the governing equations in the computational domain. The governing equations for transient study comprise of a time-dependent continuity equation for conservation of mass, three time-dependent conservation of momentum equations, and a time-dependent conservation of energy equation. Each of these equations can be expressed in a general form by the transport of a specific scalar quantity ϕ per unit mass, represented in a continuous integral form as [7]:

$$\frac{\partial}{\partial t}\int_{CV}\rho\phi dV + \oint_A \mathbf{n}.(\rho\phi\mathbf{u})dA = \oint_A \mathbf{n}.(\Gamma_\phi\nabla\phi)dA + \int_{CV} S_\phi\, dV \qquad (1)$$

Where, CV is the control volume of a three-dimensional cell, A is the surface area of the control volume, $\mathbf{n}$ is the unit outward normal vector to the surface element dA, $\mathbf{u}$ is the velocity vector and ρ is the density. The terms in equation (1), from left to right are, the rate of change the property ϕ in the control volume, the rate of change the property ϕ due to the convection flux across the boundaries of the control volume, the rate of change the property ϕ due to the diffusive flux across the boundaries of the control volume, and the source term. The source term in equation (1) contains the effects of the pressure gradient and all types of body forces. The set of transport equations is obtained by selecting appropriate expressions for the diffusion coefficient Γ_ϕ and source term S_ϕ and setting the variable ϕ in equation (1) to velocity vector components for momentum equations, and i for energy equation, where i is the internal energy of the fluid or solid. The integral form of the mass conservation equation can also be obtained from equation (1) by setting $\phi = 1$ and the source term $S_\phi = 0$.

The volume of fluid (VOF) model [8] is used to capture the movement of the interface between the phases in the water jet simulation, while a single phase flow simulation is used for the air jet. The k-ω SST model [9] is used as a turbulent model. This model solves additional transport equations for turbulent kinetic energy k and specific dissipation rate ω, from which the turbulent viscosity can be derived. The coupled approach is used to solve the CHT problem.

MODELSETUP AND VALIDATION

The computational domain with the relevant boundary conditions is shown in Figure 1. Grids independent study were carried out in the earlier stage to select the optimum mesh count. The criteria for choosing the cell count in the current study are based on the validation process, i.e., the numerical results for many grids and many parameter settings were checked and compared with experimental results. A mesh is clustered along the jet path and the wall jet, producing a dimensionless wall distance value of $y^+ < 3.0$ at the solid-fluid interface. The time step is selected to Δt = 1.0 x10^{-3}s with ten internal iterations. In the current study, the computational results are considered to have converged when the scaled residuals fall below 10^{-6}.

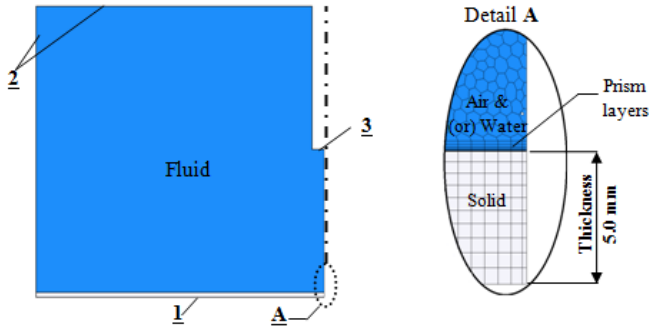

1: Constant heat flux boundary(q); 2: Pressure outlet; 3: Nozzle exit

Figure 1 Section through computational domain

A fully developed pipe flow profile with diameters of d = 12.5 and 25.0 mm for air and d = 4.0 and 6.0 mm for water are used in the current simulations. A wide range of jet's Reynolds number is employed at the nozzle exit, i.e., Re = 5000 – 30000, with nozzle-to-target spacing of H/d = 6.0 for both working fluids. However, only the results corresponding to Re = 20000 is presented in this paper. The CHT effect is investigated by using a 5.0 mm thick circular disc of diameter D = 600 mm. Three different materials are employed in the simulations, i.e., copper, aluminium and stainless steel. The physical and thermal properties of these materials are given in Table 1. The water and air physical properties are evaluated as a function of the local temperature in the computational domain. A range of constant heat flux, i.e., $q_b = 1000 - 5000$ W/m2, is employed as a thermal boundary condition for different cases in the study.

Properties / Materials	ρ (kg/m^3)	κ (W/m.K)	c_p (J/kg.K)
Cu	8940	398	386
Al	2702	237	903
316SST	7990	15.4	500

Table 1 Physical properties of the considered materials

The validation process is carried out in this study by comparing the computational results using zero plate thickness (no conjugate effect), with experimental data from [10] for the air jet problem and from [11] for the water jet problem. Figure 2 shows the validation process for the air jet with nozzle diameter d = 25.0 mm and the water jet with nozzle diameter d = 4.1 mm. A wide range of jet Reynolds numbers is used in the validation process for both cases. In these figures, the normalized local Nusselt number $\mathrm{Nu}_i/\mathrm{Nu}_0$ is plotted versus the normalized radial direction r/d using uniform heat flux boundary of $q_b = 1000\mathrm{W/m}^2$, where r is the radial distance measured from the stagnation point. The stagnation point Nusselt number (Nu_0) is used to normalize the local Nusselt number (Nu_i) profile in both figures. It is clearly shown in Figure 2 that the computational

models can reasonably replicate the experimental data with a maximum difference of less than 12%. The difference between computational and experimental results increases with the jet's Reynolds number. The maximum difference appears with the air jet simulation at Re =30000. The Nu_0 is also compared from the computational results with the ones from the experiments for different nozzle sizes (the results are not presented here). The maximum difference is less than 8%, which occurs with the water jet for $d = 6.0$ mm.

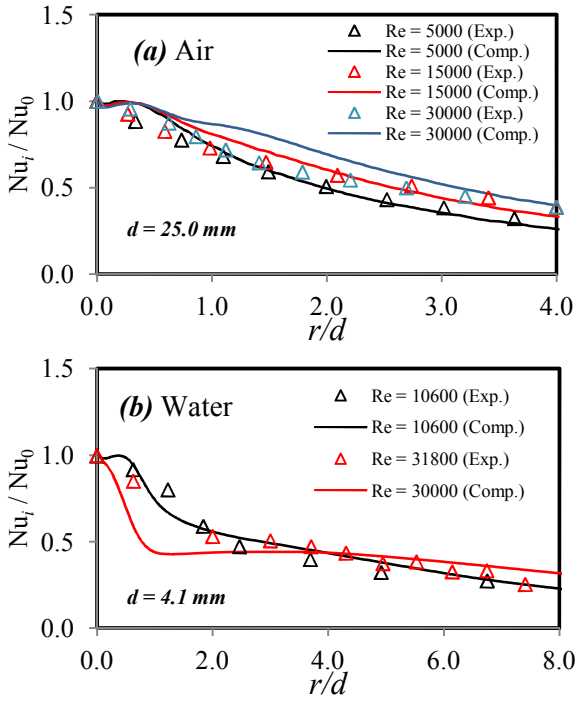

Figure 2 Comparison between computational and experimental results: (a) air jet at $H/d = 6.0$; (b) water jet at $H/d = 2.5$

RESULTS

When the solid plate has a finite thickness, the conductive heat transfer inside the solid has a significant influence on the convective heat transfer from the plate surface. The CHT process will act to redistribute the uniform boundary heat flux inside the solid and make a difference not only at stagnation, but also in the local Nusselt number [11]. As the plate thickness increases, the conductive thermal resistance in the radial direction $(R_r \, \alpha \, 1/\kappa.t_D)$ decreases, while the conductive thermal resistance in the axial direction $(R_a \, \alpha \, t_D/\kappa)$ increases. Therefore, the conductive heat transfer in the radial direction towards the impingement point increases with the plate thickness, while the conductive heat transfer in the axial direction towards the surface (interface) decrease as the plate thickness increases. The heat flux will not remain uniform at the interface as in the case of the zero plate thickness. In the convective heat transfer problem that involves a CHT process, the HTC profile at the interface depends on the thermal properties and thickness of the plate beside the other flow parameters. The effect of the CHT process on the stagnation and local Nusselt number is investigated in this using jet's Reynolds number of Re = 20000 (other jet's Reynolds numberes are also investigated but not presented here) and three uniform boundary heat fluxes, i.e., $q_b = 1500, 3000 \,\&\, 5000$ W/m^2. The physical and thermal properties of the material that used in the investigation are given in Table. 1.

Figure 3 shows the effect of the CHT process onto the $Nu_0$for different q_b with the air jet. In this figure, the non-dimensional HTC (Nu_0) is normalized by using the corresponding nozzle size and fluid thermal conductivity at the nozzle exit. For a pure convective heat transfer process (no CHT), the smaller nozzle provides better stagnation HTC due to the higher radial velocity gradient at the stagnation point [12]. Apparently, the CHT process has an effect on the Nu_0 profile, which is also influenced by the nozzle size as shown in Figure 3a &b. This is due to the dependence of the convective thermal resistance onto the nozzle size, which controls the thermal characteristics at the stagnation point. The increase of the boundary heat flux $q_b$acts to increase the temperature $T_0$and the interface heat flux q_0 (see also Figure 4) at the stagnation point. However, the increase in the temperature (ΔT_0) will be dominant over the increase in the heat flux (Δq_0), which, combined, reduces the Nu_0 as the boundary heat flux increases. The decrease in Nu_0 is more obvious for the metal with higher thermal conductivity (Cu & Al) as shown in Figure 3, where the gradient of the Nu_0 profile increases (higher negative magnitude) with the metal thermal conductivity. The Nu_0 dependence onto the q_b is less sensitive for metal with low thermal conductivity (316SST).

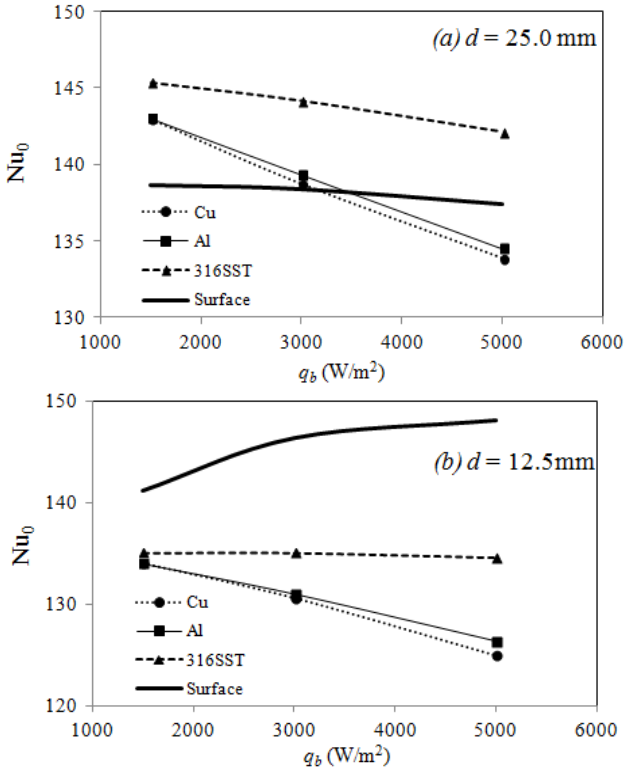

Figure 3 Effect of the CHT process on the Nu_0 for the air jet (a) d = 25.0 mm; (b) d = 12.5 mm

The CHT process enhances the interfacial heat transfer q_0 at the stagnation point for the air jet impingement process as shown in Figure 4. The nozzle size has a significant effect on the q_0, where the heat flux q_0 increases by approximately 100% for the smaller nozzle due to the higher velocity gradient compared to the larger sized nozzle. For a given nozzle size, the q_0 is governed by both components of the thermal conductive resistance, i.e. R_r and R_a. The radial thermal resistance R_r decreases faster than the increase in the axial thermal resistance R_a for the metal with high thermal conductivity (Cu & Al). This acts to enhance the conductive heat transfer inside the solid towards the stagnation point and increase the heat flux at the stagnation point. The interfacial heat flux q_0 for the metal with lower thermal conductivity (316SST) approaches the one with no CHT process as shown in Figure 4.

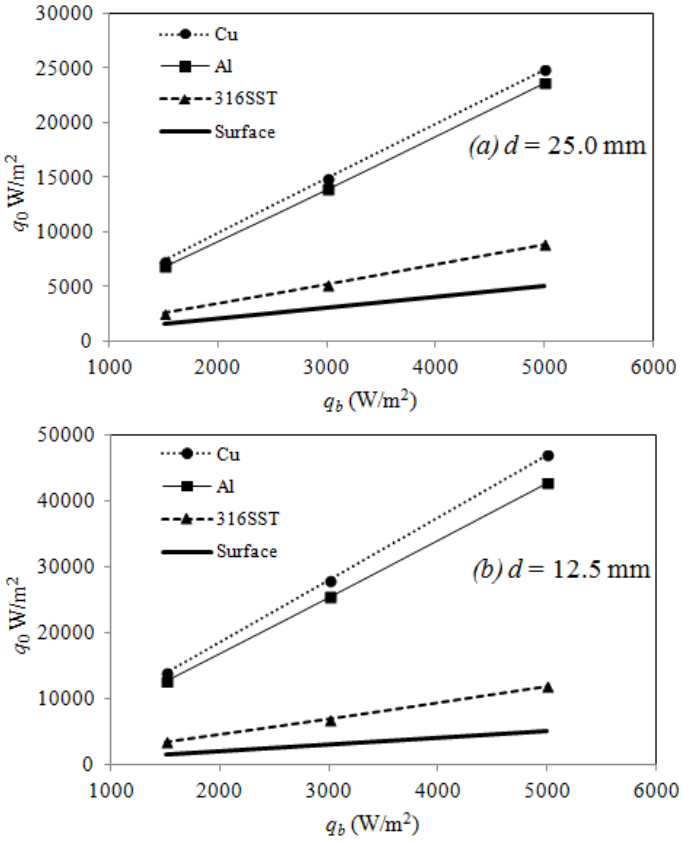

Figure 4 Effect of the CHT process on the q_0 for the air jet (a) d = 25.0 mm; (b) d = 12.5 mm

Following impingement, the flow turns and enters a wall jet region where the flow moves outward parallel to the wall. Close to the stagnation point, the fluid jet flow is strongly influenced by the wall, and is quickly decelerated in the axial direction and then accelerated in the radial directions. The wall jet characteristics due to the jet impingement are extensively discussed in [13 - 14]. The effect of the CHT process on the normalized Nusselt number $\mathrm{Nu}_i/\mathrm{Nu}_0$ is shown in Figure 5. It is obvious from this figure that the Nu_i/Nu_0 profile is more sensitive to the CHT process when the nozzle size is as large as shown in Figure 5a; where the profile with the CHT process is completely shifted below the one with no CHT process. For both nozzle sizes and at a radial distance r/d > 0.75, the $\mathrm{Nu}_i/\mathrm{Nu}_0$ profile is slightly shifted upward as the thermal conductivity of the metal decreases (316SST). Another conclusion can be drawn from Figure 5 which is that for the operating condition used in the study, i.e., nozzle size, jet's Reynolds number and disc metal, the $\mathrm{Nu}_i/\mathrm{Nu}_0$ profile is a function of the r/d only and it is independent on the boundary heat flux q_b.

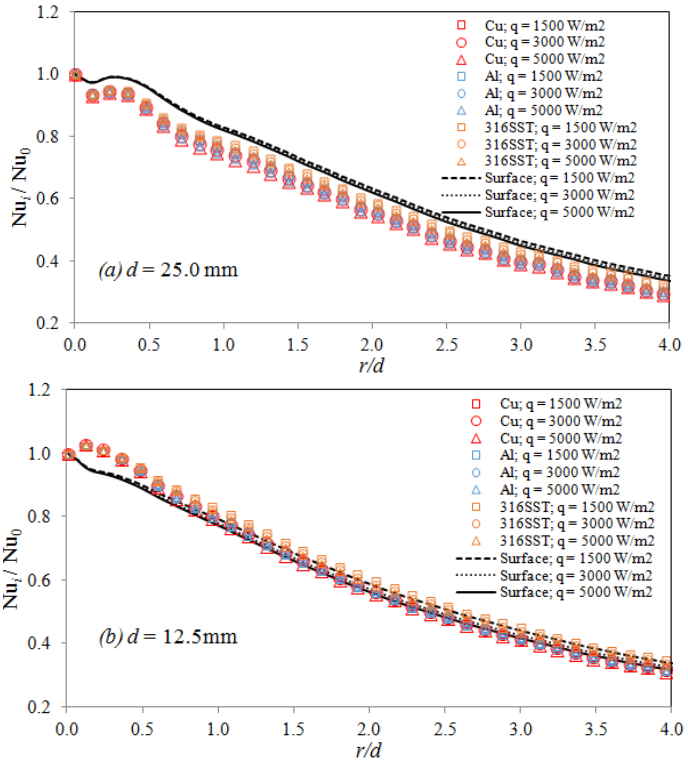

Figure 5 Effect of the CHT process onto the normalized $\mathrm{Nu}/\mathrm{Nu}_0$ profile for the air jet; (a) d = 25.0 mm, (b) d = 12.5 mm

The effect of the CHT process onto the normalized temperature distribution for the air jet is shown in Figure 6. In this figure, the interfacial local temperature T_i is normalized with the minimum temperature T_0 at the stagnation point. It is obvious from Figure 6 that the normalized profile is uniform at the interface when the thermal conductivity of the metal is high (Cu & Al) for all boundary heat fluxes q_b that are used in the study. The temperature distribution seems to be more uniform for the copper rather than aluminum due to the higher thermal conductivity of the copper. As the thermal conductivity of the metal decreases (316SST), the temperature distribution profile deviates from a uniform profile towards the one with no CHT process (surface) as shown in Figure 6. For both nozzle sizes, the normalized temperature profile is uniform in the range of $r/d \leq 0.5$ for all metals used in the study. This indicates that the metal thermal conductivity has no effect onto the normalized distribution within this range. For nozzle sizes d = 25.0 & 12.5 mm and q_b = 3000 W/m^2, the minimum

temperatures at the stagnation point are 123, 115 & 54 ˚C and 123, 113 & 44˚C for Cu, Al & 316SST, respectively.

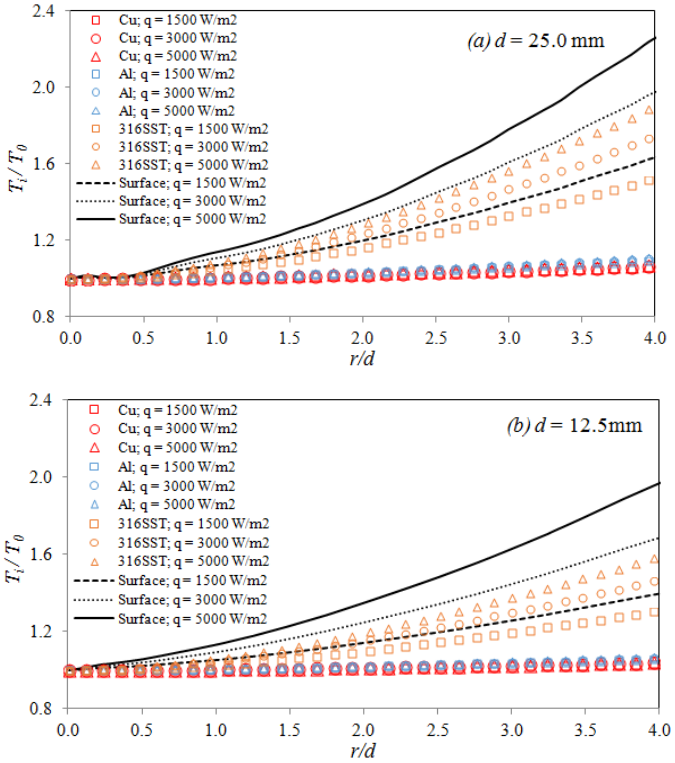

Figure 6 Effect of the CHT process onto the normalized T/T_0 profile for the air jet; (a) d = 25.0 mm, (b) d = 12.5 mm

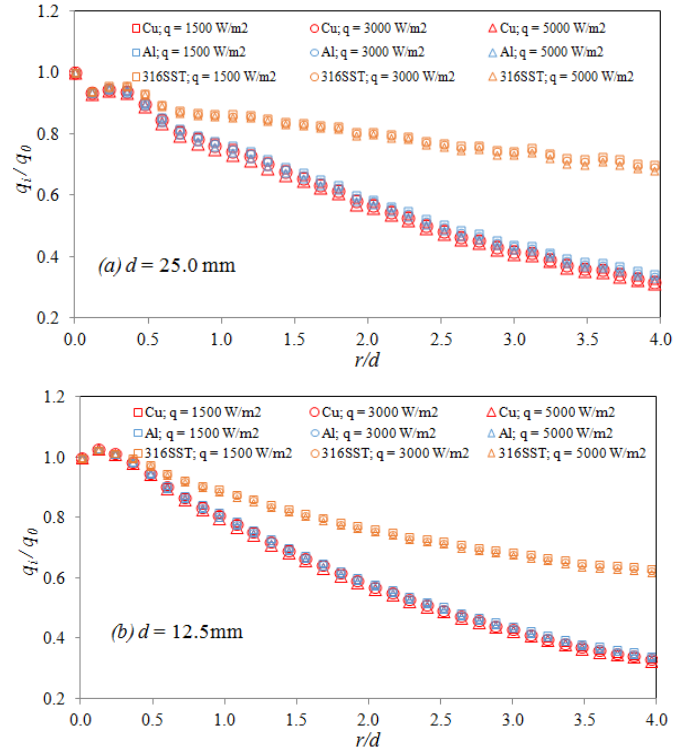

Figure 7 Effect of the CHT process onto the normalized q_i/q_0 profile for the air jet; (a) d = 25.0 mm, (b) d = 12.5 mm

The effect of the CHT process onto the normalized local interfacial heat flux distribution for the air jet is shown in Figure 7. In this figure, the local heat flux q_i is normalized with the stagnation point heat flux q_0. The profile of the interfacial heat flux is more uniform for the metal with lower thermal conductivity (316SST) and approaches the profile of no CHT process ($q_i/q_0 = 1.0$). It is clearly shown in Figure 7 that for a given metal and operating conditions, the q_i/q_0 profile is function of the radial position r/d and it is independent onto the boundary heat flux strength q_b. The profiles for all metals are identical within $r/d \leq 0.5$, i.e., at the radial distance of the nozzle edge.

Figure 8 shows the effect of the CHT process onto the Nu_0 for the water jet. Unlike the air jet (see Figure 3), the Nu_0 profile appears to be constant for both nozzle sizes and is insensitive to the conjugate process and boundary heat flux q_b. Keeping in mind that the Nusselt number has been calculated using the corresponding nozzle diameter and thermal conductivity of the working fluid, i.e.,$\kappa = 0.0257$ and 0.6 W/m.K for air and water, respectively, the HTC at the stagnation point is highest with the water jet at a nozzle size of d = 4.0 mm. The difference in the cooling (or heating) behaviour for water and air jets is attributed to the thermal characteristics of the working fluid, i.e., the heat capacity (c_p) and the Prandtl number (P_r). The heat capacity of the water is more than four times of the air one, while the Prandtl number for water is about 7.0 compared to 0.7 for air at 20 °C. Therefore the thermal diffusivity is dominant over the momentum diffusivity for the air jet and the other way for the water jet, which enhances the heat transfer coefficient for the water jet

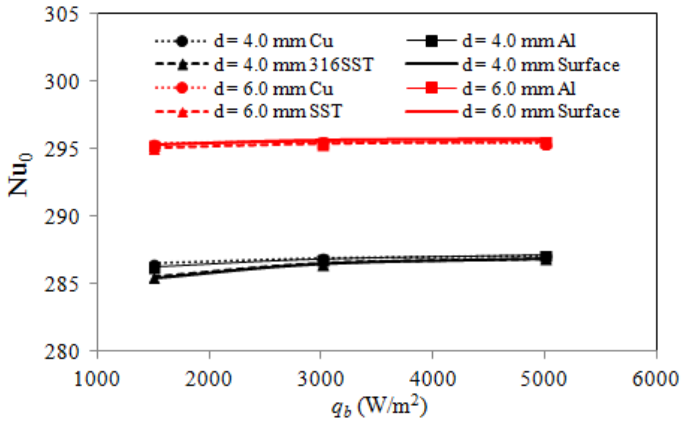

Figure 8 Effect of the CHT process on the Nu_0 for the water jet

The effect of the CHT process onto the interfacial heat transfer q_0 at the stagnation point for the water jet is given in Figure 9. It is clearly shown in this figure that the CHT process affects the heat transfer at the stagnation point compared to the one with no CHT process. The nozzle size also has an effect on the CHT process when the thermal conductivity of the metal is small (316SST), where the q_0 profiles appear below and above the profile with no CHT process as shown in Figure 9a & b, respectively. For the process including a water jet, the interfacial temperature approaches the bulk temperature of the

fluid (not presented here), which acts to reduce the $q_0$compared to the air jet impingement process (see Figure 4).

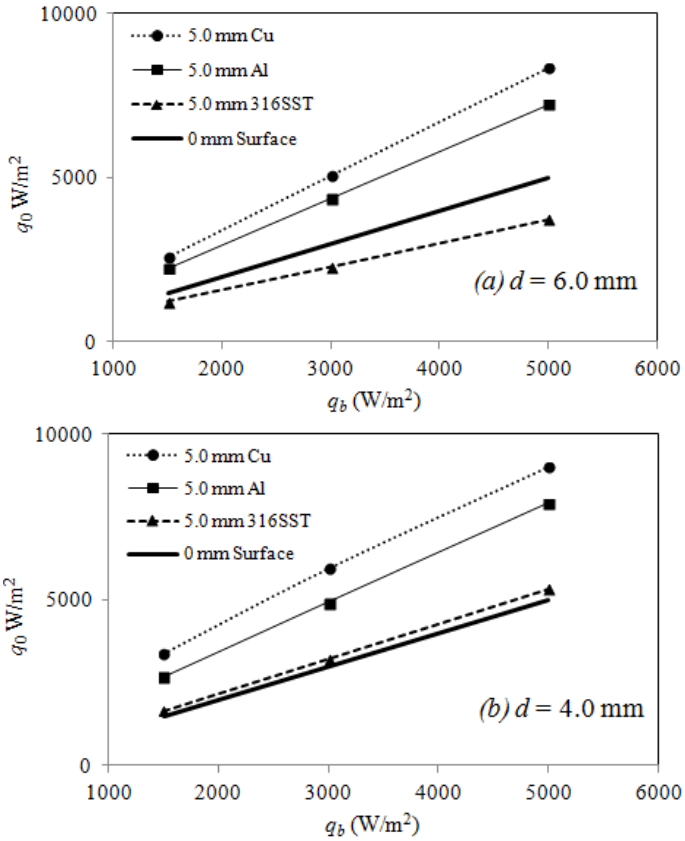

Figure 9 Effect of the CHT process on the Nu_0 for the water jet (a) d = 6.0 mm; (b) d = 4.0 mm

CONCLUSION

A numerical CHT investigation is carried out in this study using jet impingement process. Two working fluids are used in the investigation, i.e., air and water. The conclusions can be summarized as follows:

- The CHT process affects the stagnation point Nusselt number Nu_0 for the air jet. The metal thermal conductivity, nozzle size and the boundary heat flux q_b are the parameters that control the Nu_0.
- The CHT process has an insignificant effect on the stagnation point Nusselt number Nu_0 for the water jet. The nozzle size is the sole parameter that controls the Nu_0.
- For any given metal, nozzle size and jet's Reynolds number, the Nu_i/Nu_0 profile is a function of the *r/d* only and it is independent on the boundary heat flux q_b. However, the profile can be influenced by the nozzle size and jet's Reynolds number. The Nu_i/Nu_0 for the water jet wasn't presented in this paper but has the same trend of the air jet.
- The CHT process often enhances the interfacial heat flux at the stagnation point q_0 in comparison with no CHT process. The heat flux q_0 increases with the thermal conductivity of the metal.
- Depending on the metal thermal conductivity, the CHT process acts to create a uniform interfacial temperature distribution T_i/T_0 as the thermal conductivity of the metal increases and the uniform interfacial heat flux q_i/q_0 as the thermal conductivity of the metal decreases for both air and water jets (interfacial heat fluxq_i/q_0 wasn't present in this paper).

REFERENCES

[1] Radenac E., Gressier J., and Millan P., Methodology of numerical coupling for transient conjugate heat transfer, Computers & Fluids, 100, 2014, pp. 95-107.

[2] Pozzi A., and Tognaccini R., Time singularities in conjugated thermo-fluid-dynamic phenomena, J. Fluid Mechanics, 538, 2005, pp. 361-376.

[3] Pozzi A., and Tognaccini R., Coupling of conduction and convection past an impulsively started semi-infinite flat plate, Int. J. Heat and Mass Transfer, 43(7), 2000, pp. 1121-1131.

[4] Fourcher B., and Mansouri K., An approximate analytical solution to the Graetz problem with periodic inlet temperature, Int. J. Heat and Fluid Flow,18(2), 1997, pp. 229-235.

[5] Shah K., Jain A., An iterative, analytical method for solving conjugate heat transfer problems, Int. J. Heat and Mass Transfer, 90, 2015, pp. 1232-1240.

[6] CD-adapco, STAR-CCM+ V10.06.009, User Manual, 2016.

[7] Versteeg H.K., and Malalasekera W., An Introduction to Computational Fluid Dynamics: The Finite Volume Method, 2nd ed., Pearson Education Ltd., Harlow, UK, 1995.

[8] Hirt C.W., and Nichols B.D., Volume of fluid (VOF) method for the dynamics of free surfaces, J. Computational Physics, 39, 1981, pp. 201-225.

[9] Menter F.R., Two-equation eddy-viscosity turbulence modeling for engineering applications, AIAA Journal, 32(8), 1994, pp. 1598-1605.

[10] Lee J., and Lee S.J., Stagnation region heat transfer of a turbulent axisymmetric jet impingement, Experimental Heat Transfer, 12(2), 1999, pp. 137-156.

[11] J. Stevens, J., and B.W. Webb, Local heat transfer coefficients under an axisymmetric, single phase liquid Jet, J. Heat Transfer, 113(1), 1991, pp. 71-78.

[12] Nasif G., Barron R.M., and Balachandar R., Heat transfer due to an impinging jet in a confined space, J. Heat Transfer, 136(11), 2014, pp. 112202.

[13] Liu X., Gabour L.A., Lienhard J.H., Stagnation-point heat transfer during impinging of laminar liquid jets: Analysis Including Surface Tension, J. Heat Transfer, 115, 1993, pp. 99-105.

[14] Liu X., Lienhard J.H., Lombara S., Convective heat transfer by impingement of circular liquid jets, J. Heat Transfer, 113, 1991, pp. 571-582.